ACS Catalysis

Letter

pubs.acs.org/acscatalysis

Role of Silanol Group in Sn-Beta Zeolite for Glucose Isomerization and Epimerization Reactions

Neeraj Rai,[†,‡] Stavros Caratzoulas,*[,†] and Dionisios G. Vlachos[†]

[†]Catalysis Center for Energy Innovation, Department of Chemical and Biomolecular Engineering, University of Delaware, 150 Academy Street, Newark, Delaware 19716, United States

[‡]Dave C. Swalm School of Chemical Engineering, Mississippi State University, Mississippi State, Mississippi 39762, United States

Supporting Information

ABSTRACT: Density functional calculations are used to elucidate the role of the silanol group adjacent to the active site Sn metal center of the Sn-BEA zeolite in the isomerization and epimerization of glucose. We find that the silanol group plays an important role in the isomerization reaction, wherein hydride transfer and subsequent proton transfer occur in a single step with a lower energy of activation. Epimerization, on the other hand, proceeds via a mechanism similar to the Bílik mechanism and has lower activation barrier when the silanol group does not participate directly in the transition state. Our calculations indicate that cooperative effects, often encountered in enzymatic catalysis, promote hydride transfer in the isomerization reaction but not for the Bílik mechanism for epimerization.

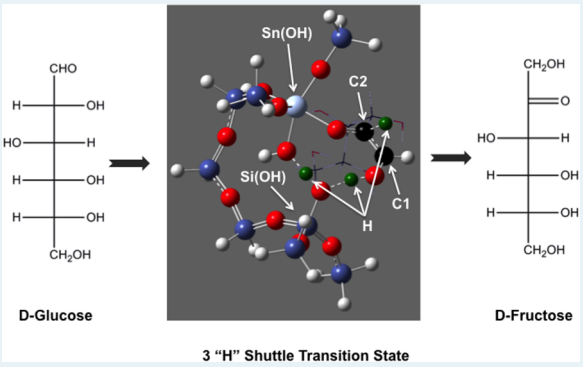

KEYWORDS: *heterogeneous catalysis, Sn-beta zeolite, isomerization, epimerization, Bílik mechanism, cooperativity*

Carbohydrates are of immense importance to fields such as nutrition science, biology and medicine, and the food industry.[1] Since only a handful of aldose and ketose sugars occur naturally and in abundant quantities, isomerization and epimerization have played a key role in carbohydrate chemistry.[1−3] However, the current worldwide emphasis on the search for carbon neutral sources of energy to meet our energy needs in a sustainable manner has reinvigorated interest in these chemical transformations. This is mainly because a large fraction of biomass consists of cellulose and hemicellulose, polymers of primarily glucose and xylose sugars, respectively.[4] The current thrust is toward breaking down lignocellulosic biomass into their constituents and subsequently converting the sugars into platform chemicals, such as 5-hydroxymethylfurfural (HMF) and furfural.[4−8] A key step in this process is aldose-to-ketose isomerization. The current industrial processes employ enzymes such as D-xylose isomerase to carry out aldose-to-ketose isomerization. However, as with any other enzymatic process, these are expensive and require precise control of process variables, such as pH, temperature, etc.[9] The search for heterogeneous catalysts that can either match or surpass enzymes in isomerization and epimerization efficiency and cost effectiveness is a highly active research area.

These efforts led to the discovery of Sn-Beta as an efficient catalyst for isomerization[9] and epimerization[10] with water and methanol as the reaction medium, respectively. In addition, Sn-Beta was shown to be active for conversion of mono- and disaccharides into methyl lactate, possibly via retro aldol condensation.[11,12] There have been several experimental and computational studies seeking to understand the mechanism of isomerization.[13−19] These studies point to an intramolecular C2−C1 hydride shift to be at play for aldose-to-ketose isomerization. In contrast, there is just a single study on the epimerization in Sn-Beta in which the authors employed ^{13}C NMR experiments and found that glucose-to-mannose epimerization in methanol proceeds via the Bílik mechanism;[10] however, it is not clear what leads to change in the product distribution (isomer to epimer) when the solvent medium is changed from water to methanol.

To date, all the evidence suggests that the active site is a partially hydrolyzed Sn site (see Figure 1c) in the Sn-Beta zeolite;[20] however, the role of the adjacent silanol group is not well understood. The majority of the experimental work in this area has focused on ^{13}C- or ^{2}H-labeled sugar molecules, which cannot resolve if the silanol groups participate directly in the key elementary reactions. Bermejo-Deval et al.[13] carried out experiments in a saturated solution of NaCl to populate adjacent silanol groups with Na^+, but these studies were inconclusive. Similarly, computational studies[13−15] have employed cluster models containing the active Sn site with and without silanol groups, but completely ignore the structural arrangement of the partially hydrolyzed Sn site and of the silanol group created as a result of the hydrolysis of the Si−O−Sn bond. While this work was under review, Yang et al.[21]

Received: June 24, 2013
Revised: September 5, 2013
Published: September 11, 2013

   dx.doi.org/10.1021/cs400476n | *ACS Catal.* 2013, 3, 2294−2298

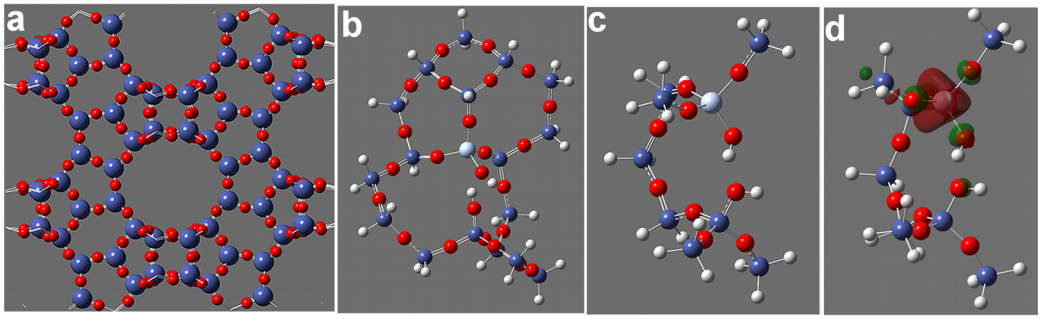

Figure 1. Construction of active site model. (a) Zeolite beta crystal, (b) the large cluster model, (c) the small active site model used in the present work, and (d) the lowest unoccupied molecular orbital is centered at the Sn atom. The dark blue, red, light blue, and white spheres show Si, O, Sn, and H atoms, respectively.

carried out periodic DFT calculations and concluded that isomerization activity can be enhanced by having a silanol nest in the vicinity of the active site.

In this Letter, we present density functional studies on isomerization and epimerization of the open form of glucose into fructose and mannose, respectively, facilitated by Sn-Beta zeolite and explore the role of adjacent silanol groups in these chemical transformations. The goal of the present work is to determine whether silanol groups can cooperatively participate in the key steps in the isomerization and epimerization reactions. The cooperative interactions between different functional groups are a hallmark of enzymatic activity,[22,23] and this concept is increasingly being applied to develop chemical catalysts[23−29] that display high selectivity and specificity.

For our work, we employed M06-2X, a hybrid meta-GGA functional developed by Zhao and Truhlar[30,31] that provides reliable thermochemistry[32] and captures the van der Waals interactions anticipated to play a role in the present work. The LANL2DZP basis set[33,34] was used for Sn and Si atoms, and 6-31+G** for H, O, and C atoms.[35−37] For the hydrogen atoms used to satisfy silicon dangling bonds, 6-31G basis functions were used. These basis sets were downloaded from the EMSL basis set exchange.[38,39] All the calculations were performed with the Gaussian 09 software suite, rev. C.[40] The ultrafine grid was used in all the calculations, and minima and transition states were verified by frequency calculations (sample input files are provided in the Supporting Information). Geometry minima are characterized by the absence of imaginary frequencies and transition states by the presence of a single imaginary frequency. Furthermore, a path along the intrinsic reaction coordinate was followed to ensure that the transition state connects the reactants and products. All electronic energies (kcal/mol) are referenced to the sum of cluster and closed form glucose molecules at infinite separation. Because the goal of the present work is to explore different reaction pathways, vibrational corrections were not applied to the energies to avoid spurious effects due to the large number of low-frequency modes in the system considered in the present study.

Following the work of Boronat et al.,[20] we built the active model around the T9 crystallographic site in the zeolite Beta in a stepwise manner (see Figure 1). In the first step, a significantly large cluster was cut out from the zeolite structure (Figure 1b). All the dangling bonds were satisfied by H atoms. The geometry was optimized with PM6[41] keeping H atoms frozen. Subsequently, the cluster was further reduced in size while maintaining the structural integrity of the partially hydrolyzed Sn site (Figure 1c). At this stage, the cluster model consisted of 49 atoms with 8 Si, 1 Sn, 10 O, and 20 H atoms, and optimizations were carried out using the M06-2X density functional. Every time a dangling bond was satisfied by adding an H atom, first, an optimization was carried out keeping these hydrogen atoms free and heavy atoms frozen. For subsequent geometry optimizations and transition state searches, these H atoms were frozen, and all other atoms were allowed to relax. The key difference from prior computational work[13−15,20] is our careful construction of the active site model to preserve the structural proximity of the Sn hydroxyl and silanol groups. The cluster model, although large, does not allow studying the confinement effects due to the zeolite framework. However, we believe that "physical" stabilization or destabilization of the transition state due to the zeolite framework would be somewhat similar to that of the intermediates connected by the transition state. Thus, the confinement effects would be smaller on the activation energies because the effect of a somewhat "rigid" framework will cancel out when we compute the differences. Furthermore, the nonadditive "chemical" effects on the transition state originate from the active site and nearby framework, which we have included in the cluster employed for the present calculation. Figure 1d shows that the lowest unoccupied molecular orbital is located at the Sn site, indicating the preferred binding site for sugar molecules.

The glucose-to-fructose isomerization involves three steps:[14,15] (a) proton transfer from the glucose molecule to the Sn−OH, (b) hydride transfer from the C2 carbon position to the C1 position, and (c) proton transfer back to the keto form of the sugar. For these steps, two different binding modes were considered. In the first case, glucose binds so that the carbonyl group is hydrogen-bonded to the silanol group (top row in Figure 2), whereas in the second case, glucose binds in a bidentate mode to the Sn site (bottom row in Figure 2). The base-catalyzed proton transfer in the first step is common to both the glucose-to-fructose isomerization and the glucose-to-mannose epimerization processes. For the Bílik reaction, instead of a hydride transfer from the C2 carbon to the C1 carbon, there is a simultaneous C1−C3 bond formation and C2−C3 bond cleavage, followed by proton transfer from the $Sn(OH_2)$ moiety back to the deprotonated form of mannose. To our knowledge, there has not been a computational study to explore the Bílik mechanism in sugar molecules.

The binding mode in which the glucose carbonyl oxygen is hydrogen-bonded to the silanol group is energetically more favorable compared with the case when it is bound to the Sn

dx.doi.org/10.1021/cs400476n | ACS Catal. 2013, 3, 2294−2298

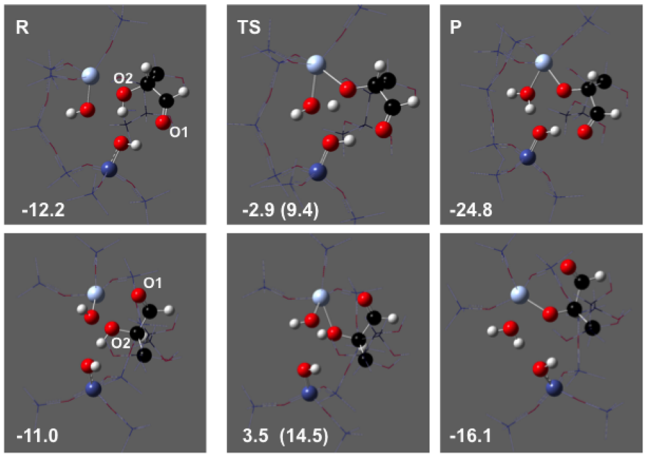

Figure 2. Structure and energetics for reactants (R, left), transition state (TS, center), and products (P, right) for proton transfer from glucose to the active Sn hydroxyl site. (Top) SiOH direct participation in the transition state, glucose binds to the Sn site in a monodentate mode. (Bottom) SiOH spectator, glucose binds to the Sn site in a bidentate mode. The numbers show energies (kcal/mol) for the species, and the numbers in the parentheses are the activation energies (kcal/mol). For clarity only, the Sn hydroxyl, silanol, C1, C2, O1, O2, H1, and H2 are shown in ball and stick representation, and rest of the cluster and glucose molecule is shown with the wireframe representation. The carbon atoms are represented by black spheres, and the color scheme for the rest of the atoms is the same as Figure.1.

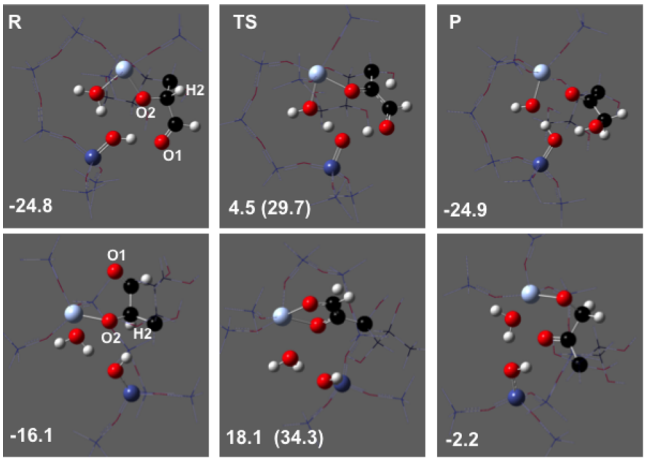

Figure 3. Structure and energetics for reactants (R, left), transition state (TS, center), and products (P, right) for the hydride transfer in glucose-to-fructose isomerization. (Top) SiOH direct participation in the transition state, glucose binds to the Sn site in a monodentate mode. (Bottom) SiOH spectator, glucose binds to the Sn site in a bidentate mode. The numbers have the same meaning as in Figure 2.

atom (in bidentate mode) by ∼1 kcal/mol (Figure 2). However, the activation energy for the proton transfer is significantly lower (≈ 5 kcal/mol) in the first case compared with the bidentate binding mode. This suggests that although the initial binding energies are comparable in the both cases, proton transfer facilitated by direct participation of the silanol group is much more probable than in the bidentate binding mode. Furthermore, the configuration of products in the former case is much more stable (by ∼9 kcal/mol) than in the latter case of bidentate mode.

The configurations and energetics for the hydride transfer (step 2 in the overall process) are shown in Figure 3. For the hydride transfer from the C2 to the C1 carbon, it appears that the proximity of the silanol group provides immense synergistic effects. This is evident from the fact that not only is the activation significantly lower, but also the proton transfer back to the sugar molecule is completed in a concerted single step. This type of cooperativity is quite common in the case of enzymatic systems, and our calculations show that similar synegistic effects may be in play in the case of the Sn-Beta zeolite, as well. The transition state involves three different hydrogen atoms that move in a concerted manner. The hydride transfer from the C2 to the C1 carbon makes the O1 oxygen significantly more negative, thereby making it a stronger Brønsted base than the silanol group. As a result, it pulls the hydrogen atom from the silanol group, which in turn pulls the hydrogen atom from the $Sn(OH_2)$ moiety and completes the isomerization in a single step.

In an earlier publication,[15] we concluded that the H transfer from C2 to C1—formally described as a hydride transfer—follows a neutral H atom-coupled electron transfer mechanism. In the current system, natural population analysis supports the same mechanism. The charge on the H atom that migrates from C2 to C1 changes from 0.253 in the reactant state to 0.328 in the transition state, indicating that the C2-to-C1 H transfer is not hydridic in nature, because that would formally entail a negative charge on the hydrogen. In the transition state, the electron is delocalized between the O2 and O1 oxygen atoms. On the other hand, the concurrent hydrogen transfers from the Sn ligand water to the silanol of the hydroxylated site and from the silanol to the O1 oxygen of the sugar are, in fact, proton transfers. Influenced by the previous work on titanium silicates by Khow and Davis,[42] Bermejo-Deval et al.[13] designed an experimental setup in which silanol groups were deprotonated and coordinated by Na^+ ions, but it did not seem to have any effect on the reaction. We believe that this could be due in part to the presence of water molecules that solvate the Na^+ ions and could show behavior similar to the silanol group. Furthermore, it can be difficult to maintain the silanol group in the deprotonated state in an acidic medium.

Encouraged by the synergistic role played by the silanol group in the isomerization reaction, we carried out a similar study for the glucose-to-mannose epimerization reaction. Bermejo-Deval et al.[13] have shown that Sn-Beta can catalyze the epimerization reaction when methanol is used as the reaction medium. ^{13}C NMR spectroscopy points to carbon−carbon bond scrambling similar to that observed in the case of the Bílik reaction[43] in molybdic acid solutions. To our surprise, we find that although the direct involvement of the silanol group in the transition state results in the epimerization process being complete in a single step, the energetic barrier is significantly higher when compared with the bidentate mode, in which the complete epimerization proceeds in the traditional two-step process (see Figure 4). The higher activation energy barrier almost makes the epimerization an unlikely reaction pathway. We believe that the constraints due to the bidentate mode binding promote the C1−C3 bond formation and C2−C3 bond scission. When methanol is used as the solvent medium, it is possible that silanol groups will be methoxylated, thereby promoting the bidentate binding mode, which results in the epimerization reaction, to be more favorable than the isomerization reaction. Our preliminary reaction free energy calculations suggest that methoxylation of silanol or stannanol is equally probable, and the methoxylated cluster has a lower free energy, ∼−0.5 kcal/mol. Thus, from a purely thermody-

dx.doi.org/10.1021/cs400476n | ACS Catal. 2013, 3, 2294−2298

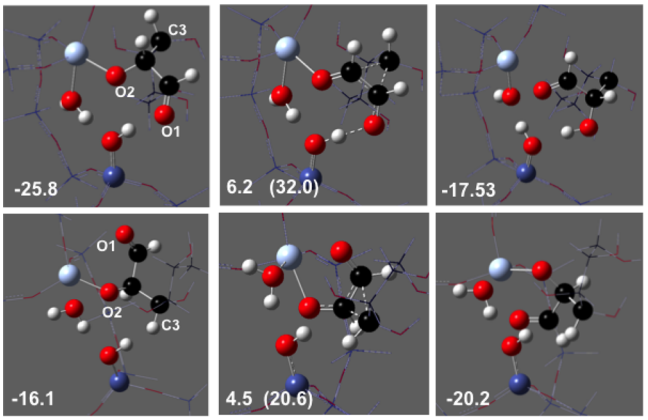

Figure 4. Structure and energetics for reactants (left), transition state (center), and products (right) for the Bílik type rearrangement for glucose to mannose epimerization. The subfigure arrangement and numbers have the same meaning as in Figure 2.

namic perspective, methoxylation is feasible, as observed by Wang et al.;[44] however, the methoxylation activation energy barriers can be different for Sn−OH and Si−OH. The subsequent methoxylation which results in both stannanol and silanol being methoxylated has substantially higher free energy, ∼10 kcal/mol.

Figure 5 shows the proton transfer back to the sugar molecule from the active Sn site. The energetic barrier for the

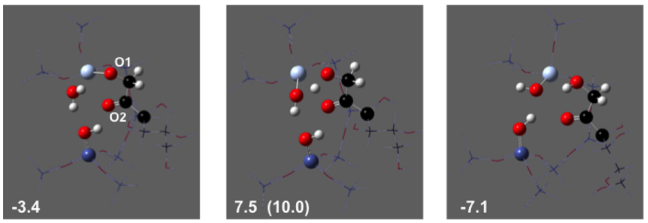

Figure 5. Structure and energetics for reactants (left), transition state (center), and products (right) for proton transfer back to fructose (from the $Sn(OH_2)$ moiety). The numbers have the same meaning as in Figure 2.

proton transfer is 10 kcal/mol and is similar to that of the initial proton transfer step. The proton transfer back to the sugar molecules, in the case of the bidentate mode, is somewhat higher, at 17 kcal/mol, and follows a transition state similar to that of the isomerization reaction. Overall, the energetic barriers for proton transfer are smaller than either the hydride transfer for the isomerization reaction or the carbon skeleton rearrangement in the case of the Bílik type mechanism for the epimerization, consistent with the NMR experiments.[13]

In summary, our calculations suggest that the silanol group adjacent to the active Sn hydroxyl site in Sn-Beta promotes, synergistically, the hydride transfer in the isomerization of glucose to fructose. We find that when the silanol group participates directly in the hydride transfer step, the isomerization is complete in a single step with lower activation energy barrier (see Table 1). For the epimerization reaction, although the key C1−C3 bond formation, C1−C2 bond scission and subsequent proton transfer back to the sugar molecule are completed in a single step, the energy barrier to this pathway is almost 11 kcal/mol higher than the case when silanol is not directly involved in the transition state. Our study indicates that

Table 1. Activation Energies in kcal/mol for Isomerization and Epimerization Reactions[a]

	HT			Bílik	
mechanism	PTI	HT	PTB	Bílik	PTB
A	9.4	29.7		32.0	
	(6.6)	(26.3)		(30.2)	
B	14.5	34.4	10.0	20.6	17.2
	(12.6)	(31.6)	(8.1)	(19.7)	(14.4)

[a]The numbers in parentheses are based on the enthalpy. [b]PTI, initial protron transfer to the silanol; HT, hydride transfer step; PTB, proton transfer back to the sugar molecule; mechanism; A, when silanol is directly participating in the transition state; B, when silanol is spectator.

hydride transfer for the isomerization reactions can significantly benefit from the cooperative effects of the silanol group, similar to an enzymatic processes. However, for the Bílik type rearrangement, it seems beneficial to have sugar molecules bound to the active site in a bidentate mode, and thus, the absence of a silanol group, via solvent selection, could enhance the epimerization rate. Furthermore, we believe that the polarity of the solvent can also affect the reaction pathway that the system could follow. The isomerization reaction involves a hydride transfer and two concomitant proton transfers; hence, the isomerization transition state is a very polarized state. On the other hand, the Bilik transition state involves the breaking of a C−C bond and the formation of another and, thereby, is less polarized. Thus, we believe that the isomerization transition state should be greatly stabilized in a polar environment. However, because methanol is not as polar as water, the presence of methanol (strictly as adsorbed solvent molecules in the vicinity of the active site) or the possible methoxylation of the stannanol or silanol groups provides a less polar (local) environment that is not as conducive to the formation of a polarized transition state complex. Our current efforts are targeted at quantifying these solvation effects.

■ ASSOCIATED CONTENT

Supporting Information

A zip file containing machine-readable sample input files, structures in *xyz* format for the geometries used in the figures and corresponding electronic energies, a movie showing transfer of hydrogen atom from the C2 to the C1 position for the concerted mechanism and geometries in *xyz* format along the IRC for this step, and a pdf file containing a figure showing the vector corresponding to the imaginary frequency for hydride transfer transition state. This material is available free of charge via the Internet at http://pubs.acs.org/.

■ AUTHOR INFORMATION

Corresponding Author

*E-mail: cstavros@udel.edu.

Notes

The authors declare no competing financial interest.

■ ACKNOWLEDGMENTS

This work was financially supported by the Catalysis Center for Energy Innovation, an Energy Frontier Research Center funded by the U.S. Department of Energy, Office of Science, Office of Basic Energy Sciences under Award No. DE-SC0001004. This research used resources of the National Energy Research Scientific Computing Center, which is supported by the Office

of Science of the U.S. Department of Energy under Contract No. DE-AC02-05CH11231.

REFERENCES

(1) Angyal, S. J. In *Glycoscience*; Stütz, A. E., Ed.; Topics in Current Chemistry; Springer: Berlin, Heidelberg, 2001; Vol. *215*; pp 1−14.
(2) Petruś, L.; Petrušová, M.; Hricovíniová, Z. In *Glycoscience*; Stütz, A. E., Ed.; Topics in Current Chemistry; Springer: Berlin, Heidelberg, 2001; Vol. *215*; pp 15−41.
(3) Häusler, H.; Stütz, A. E. In *Glycoscience*; Stütz, A. E., Ed.; Topics in Current Chemistry; Springer: Berlin, Heidelberg, 2001; Vol. *215*; pp 77−114.
(4) Huber, G. W.; Iborra, S.; Corma, A. *Carbohydr. Res.* **2006**, *106*, 4044−4098 PMID: 16967928.
(5) Román-Leshkov, Y.; Chheda, J. N.; Dumesic, J. A. *Science* **2006**, *312*, 1933−1937.
(6) Chheda, J. N.; Roman-Leshkov, Y.; Dumesic, J. A. *Green Chem.* **2007**, *9*, 342−350.
(7) Corma, A.; Iborra, S.; Velty, A. *Carbohydr. Res.* **2007**, *107*, 2411−2502.
(8) Zakrzewska, M. E.; Bogel-Lukasik, E.; Bogel-Lukasik, R. *Carbohydr. Res.* **2011**, *111*, 397−417.
(9) Moliner, M.; Roman-Leshkov, Y.; Davis, M. E. *Proc. Natl. Acad. Sci. U.S.A.* **2010**, *107*, 6164−6168.
(10) Bermejo-Deval, R.; Gounder, R.; Davis, M. E. *ACS Catal.* **2012**, *2*, 2705−2713.
(11) Holm, M. S.; Saravanamurugan, S.; Taarning, E. *Science* **2010**, *328*, 602−605.
(12) Holm, M. S.; Pagan-Torres, Y. J.; Saravanamurugan, S.; Riisager, A.; Dumesic, J. A.; Taarning, E. *Green Chem.* **2012**, *14*, 702−706.
(13) Bermejo-Deval, R.; Assary, R. S.; Nikolla, E.; Moliner, M.; Román-Leshkov, Y.; Hwang, S.-J.; Palsdottir, A.; Silverman, D.; Lobo, R. F.; Curtiss, L. A.; Davis, M. E. *Proc. Natl. Acad. Sci. U.S.A.* **2012**, *109*, 9727−9732.
(14) Assary, R. S.; Curtiss, L. A. *J. Phys. Chem. A* **2011**, *115*, 8754−8760.
(15) Choudhary, V.; Caratzoulas, S.; Vlachos, D. G. *Carbohydr. Res.* **2013**, *368*, 89−95.
(16) Roman-Leshkov, Y.; Davis, M. E. *ACS Catal.* **2011**, *1*, 1566−1580.
(17) Román-Leshkov, Y.; Moliner, M.; Labinger, J. A.; Davis, M. E. *Angew. Chem., Int. Ed.* **2010**, *49*, 8954−8957.
(18) Gounder, R.; Davis, M. E. *ACS Cat.* **2013**, *3*, 1469−1476.
(19) Choudhary, V.; Pinar, A. B.; Sandler, S. I.; Vlachos, D. G.; Lobo, R. F. *ACS Catal.* **2011**, *1*, 1724−1728.
(20) Boronat, M.; Concepción, P.; Corma, A.; Renz, M.; Valencia, S. *J. Catal.* **2005**, *234*, 111−118.
(21) Yang, G.; Pidko, E. A.; Hensen, E. J. M. *ChemSusChem* **2013**, DOI: 10.1002/cssc.201300342.
(22) Brady, L.; Brzozowski, A. M.; Derewenda, Z. S.; Dodson, E.; Dodson, G.; Tolley, S.; Turkenburg, J. P.; Christiansen, L.; Hugejensen, B.; Norskov, L.; Thim, L.; Menge, U. *Nature* **1990**, *343*, 767−770.
(23) Swiegers, G. F.; Chen, J.; Wagner, P. *Bioinspiration and Biomimicry in Chemistry*; John Wiley & Sons, Inc.: New York, 2012; pp 165−208.
(24) Konsler, R. G.; Karl, J.; Jacobsen, E. N. *J. Am. Chem. Soc.* **1998**, *120*, 10780−10781.
(25) Brunelli, N. A.; Didas, S. A.; Venkatasubbaiah, K.; Jones, C. W. *J. Am. Chem. Soc.* **2012**, *134*, 13950−13953.
(26) Kubota, Y.; Goto, K.; Miyata, S.; Goto, Y.; Fukushima, Y.; Sugi, Y. *Chem. Lett.* **2003**, *32*, 234−235.
(27) Zeidan, R. K.; Hwang, S.-J.; Davis, M. E. *Angew. Chem., Int. Ed.* **2006**, *45*, 6332−6335.
(28) Delferro, M.; Marks, T. J. *Carbohydr. Res.* **2011**, *111*, 2450−2485.
(29) Madhavan, N.; Jones, C. W.; Weck, M. *Acc. Chem. Res.* **2008**, *41*, 1153−1165.
(30) Zhao, Y.; Truhlar, D. *Theor. Chem. Acc.* **2008**, *120*, 215−241.
(31) Zhao, Y.; Truhlar, D. G. *Acc. Chem. Res.* **2008**, *41*, 157−167.
(32) Linder, M.; Brinck, T. *Phys. Chem. Chem. Phys.* **2013**, *15*, 5108−5114.
(33) Wadt, W. R.; Hay, P. J. *J. Chem. Phys.* **1985**, *82*, 284−298.
(34) Check, C. E.; Faust, T. O.; Bailey, J. M.; Wright, B. J.; Gilbert, T. M.; Sunderlin, L. S. *J. Phys. Chem. A* **2001**, *105*, 8111−8116.
(35) Hehre, W. J.; Ditchfield, R.; Pople, J. A. *J. Chem. Phys.* **1972**, *56*, 2257−2261.
(36) Hariharan, P.; Pople, J. *Theor. Chim. Acta* **1973**, *28*, 213−222.
(37) Clark, T.; Chandrasekhar, J.; Spitznagel, G. W.; Schleyer, P. V. R. *J. Comput. Chem.* **1983**, *4*, 294−301.
(38) Feller, D. *J. Comput. Chem.* **1996**, *17*, 1571−1586.
(39) Schuchardt, K. L.; Didier, B. T.; Elsethagen, T.; Sun, L.; Gurumoorthi, V.; Chase, J.; Li, J.; Windus, T. L. *J. Chem. Inf. Model.* **2007**, *47*, 1045−1052.
(40) Frisch, M. J.; Trucks, G. W.; Schlegel, H. B.; Scuseria, G. E.; Robb, M. A.; Cheeseman, J. R.; Scalmani, G.; Barone, V.; Mennucci, B.; Petersson, G. A.; Nakatsuji, H.; Caricato, M.; Li, X.; Hratchian, H. P.; Izmaylov, A. F.; Bloino, J.; Zheng, G.; Sonnenberg, J. L.; Hada, M.; Ehara, M.; Toyota, K.; Fukuda, R.; Hasegawa, J.; Ishida, M.; Nakajima, T.; Honda, Y.; Kitao, O.; Nakai, H.; Vreven, T.; Montgomery, J. A.; Peralta, J. E.; Ogliaro, F.; Bearpark, M.; Heyd, J. J.; Brothers, E.; Kudin, K. N.; Staroverov, V. N.; Kobayashi, R.; Normand, J.; Raghavachari, K.; Rendell, A.; Burant, J. C.; Iyengar, S. S.; Tomasi, J.; Cossi, M.; Rega, N.; Millam, J. M.; Klene, M.; Knox, J. E.; Cross, J. B.; Bakken, V.; Adamo, C.; Jaramillo, J.; Gomperts, R.; Stratmann, R. E.; Yazyev, O.; Austin, A. J.; Cammi, R.; Pomelli, C.; Ochterski, J. W.; Martin, R. L.; Morokuma, K.; Zakrzewski, V. G.; Voth, G. A.; Salvador, P.; Dannenberg, J. J.; Dapprich, S.; Daniels, A. D.; Farkas, O.; Foresman, J. B.; Ortiz, J. V.; Cioslowski, J.; Fox, D. J. *Gaussian 09 Revision C.1*. Gaussian Inc.: Wallingford, CT, 2009.
(41) Stewart, J. *J. Mol. Model.* **2007**, *13*, 1173−1213.
(42) Khouw, C.; Davis, M. *J. Catal.* **1995**, *151*, 77−86.
(43) Hricovíniová, Z.; Hricovíni, M.; Petrušová, M.; Serianni, A. S.; Petruś, L. *Carbohydr. Res.* **1999**, *319*, 38−46.
(44) Wang, W.; Seiler, M.; Hunger, M. *J. Phys. Chem. B* **2001**, *105*, 12553−12558.